coustics'08
Paris
June 29-July 4, 2008
www.acoustics08-paris.org

# Improvements of a parametric model for fan broadband and tonal noise

Antoine Moreau and Lars Enghardt

DLR - German Aerospace Center, Mueller-Breslau-Str. 8, 10623 Berlin, Germany
antoine.moreau@dlr.de

Engine fan noise is one of the dominant noise sources of civil aircraft. The purpose of the present work is to develop a tool for fan noise prediction which can be integrated into the design process of innovative fans. Fan noise is predicted here by means of analytical models. The rotor-stator interaction noise due to rotor blade wakes impinging onto the stator vanes is the single noise source mechanism considered in this first approach. This source is known to be the major contributor to tonal noise and broadband noise. The model provides a sound power spectrum that includes both the broadband and tonal components and an advanced description of the sound field based on acoustic duct modes over the whole range of fan operating conditions.

# 1 Motivations

Engine noise is a major constraint for the design of future environmentally friendly civil aircraft. Therefore it is necessary to integrate its prediction into the design process of future aero-engines - the so called „design-to-noise" approach. The work presented in this paper is part of a project among DLR aiming at developing a tool for fan noise prediction. It is the continuation of a previous study presented by the authors [1].

Fig.1 presents the three approaches utilized by the scientific community to develop new engines: experiments, numerical simulations and prediction. Prediction consists in decomposing the global system - the engine - into elementary sub-systems, which are described by simple models capturing the relevant physical mechanisms. The behaviour of the global system is obtained through the assembling of the sub-systems. The use of simplified models allows for markedly reduced computation time, which in turn makes it possible to investigate a large number of engine parameters and to assess their impact on global engine performance.

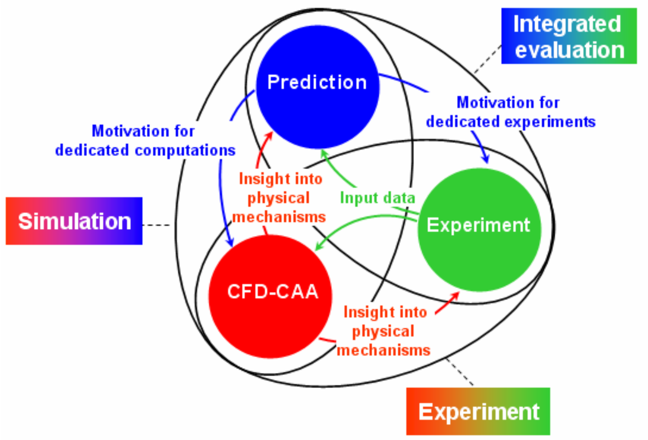


Fig.1: Research methodology for future engine design.

# 2 Description of the fan noise model

Compared to the fan noise model developed previously by Heidmann [2], the investigation of various fan configurations (high-bypass-ratio fan, contra-rotating fan, open rotor) will be possible using the model described hereafter.

## 2.1 Structure of the tool

The present tool is structured into distinctive modules which can be exchanged and/or modified depending on the fan configuration investigated. The input data needed for the noise generation are determined by analytical aerodynamic models. Moreover, an advanced description of the sound field through duct modes has been implemented, which enables to account for particular source distributions and to assess the transmission into the far field, the liner attenuation and the transmission through blade rows.

As shown in Figures 2 and 3, the tool is structured in three separate modules dedicated to noise generation, propagation and radiation, respectively. Several noise sources can be implemented independently. Pre-processing modules ("steady aero." and "unsteady aero.") based on analytical aerodynamic models provide the acoustic models with the required aerodynamic input data.

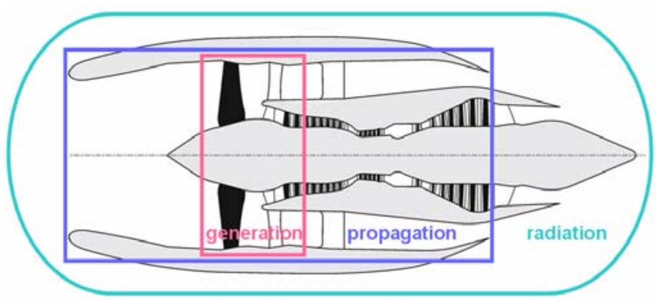


Fig.2: Typical turbofan engine in use on civil aircrafts.

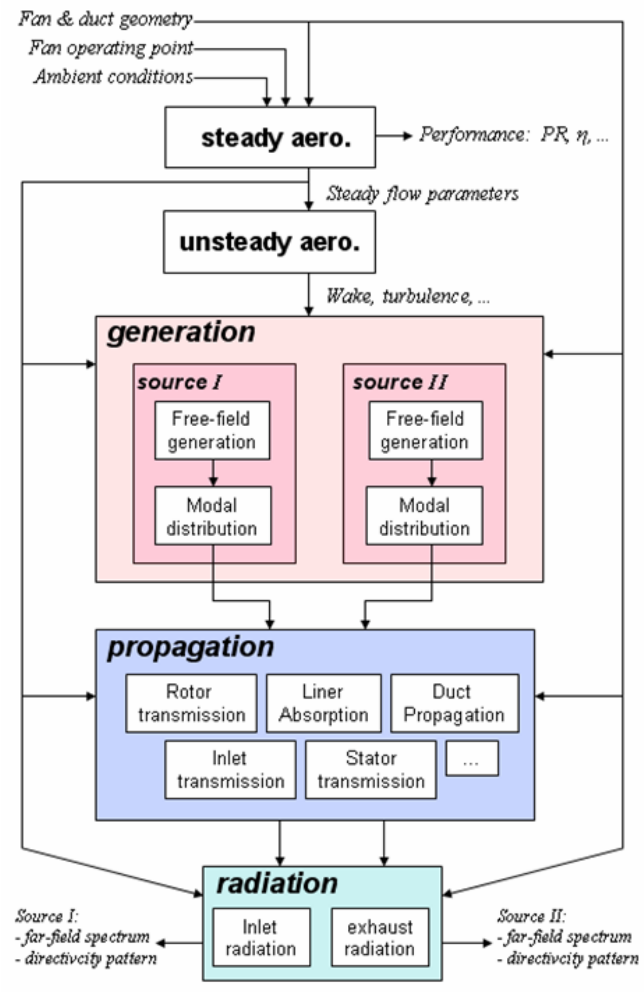


Fig.3: Structure of the DLR fan noise prediction tool.

## 2.2 Noise generation

Sound generation is caused by the unsteady flow fluctuations. Therefore these are relevant inputs for the noise model. The velocity fluctuations are computed by the "unsteady aero." module from the steady flow velocities, which are provided by the "steady aero." module. Noise generation is computed in two steps: i) the noise generation is assessed for non-interfering single airfoils in free field and ii) the source interference and duct confinement effects are considered in a second step (see section 2.3). The free-field model is derived from Amiet´s theory [3]. It accounts for subsonic compressible flow and source non-compactness.

The source modelled here is the rotor-stator interaction noise: the wakes of the rotor blades impinge onto the stator vanes and generate tonal noise at the harmonics of the blade passing frequency (BPF) and also broadband noise. This source is known to be a dominant noise generation mechanism for subsonic fans of modern aero-engines along with rotor self-noise.

Formulae for the free-field tonal sound power and for the free-field broadband sound power spectral density are given in Equations (1) and (2), respectively.

$$P^{I}(h) = a \cdot V \cdot \rho_0 \cdot c_0^3 \cdot S \cdot [k \cdot c]^2 \cdot \left[M_0^2 \cdot G(\sigma)\right]^2 \cdot \left[\frac{u_{per}(h)}{U_0}\right]^2 \quad (1)$$

$$P^{II}(St) = b \cdot V \cdot \rho_0 \cdot c_0^3 \cdot S \cdot [k \cdot c]^2 \cdot \left[M_0^2 \cdot G(\sigma)\right]^2 \cdot \left[\frac{u_{turb}(St)}{U_0}\right]^2 \quad (2)$$

$a$, $b$: empirical coefficients.
$St$: Strouhal number based on the integral length scale of stator inflow turbulence.
$h$: harmonics of the rotor blade passing frequency.
$k$: acoustic wave number.
$S$: duct section area at stator station.
$V$, $c$: stator vane count, stator vane chord length.
$G(\sigma)$: compressible Sears function (see [3] and [4]).
$\sigma$: Sears non-dimensional frequency.
$\rho_0$, $c_0$, $M_0$, $U_0$: air density, sound speed, Mach number and velocity magnitude of stator inflow.
$u_{turb}(St)$, $u_{per}(h)$: turbulent and periodic wake velocity spectra of stator inflow.
Remark: $P^{II}(St)$ and $u_{turb}(St)$ are spectral densities.

## 2.3 Modal distribution

The sound scattering due to duct confinement is accounted for when the noise source is modelled by a set of point sources distributed along the stator vane leading edges. This source distribution can in turn be related to duct modes through the duct Green´s function. Equations (3) and (4) yield the modal power distribution $P_{mn}$ given the free-field sound power $P$.

$$P_{mn}{}^{I} = H_{mn}{}^{I} \cdot P^{I} \quad (3)$$

$$P_{mn}{}^{II} = H_{mn}{}^{II} \cdot P^{II} \quad (4)$$

$H_{mn}{}^{I}$ and $H_{mn}{}^{II}$ are the modal duct transfer functions for tonal and broadband noise, respectively. They are computed for a given distribution of sound sources by means of the duct Green´s function for a hollow, hard-walled duct without flow. Details for computing this function are given by Rienstra [5]. The modal duct transfer functions are sensitive to the location, amplitude and phase of the sources.

For tonal noise we assume a uniform radial distribution of correlated monopoles located on the stator vane leading edges. The vane-to-vane phase shift is set by the delay of rotor wakes impinging onto the vanes and is therefore consistent with the Tyler & Sofrin theory [6]. For broadband noise we consider a uniform radial distribution of uncorrelated monopoles located on the stator vane leading edges.

This decomposition of the sound field into modes allows for considering the effect of the different parts of the duct: for example, the transmission through a blade row or the influence of a lined section. In the present study it is utilized to assess the transmission into the far-field.

## 2.4 Transmission into the far field

The sound transmission at the duct openings into the far field is computed at the different frequency lines for each mode ($m$,$n$) propagating in the duct. The transmitted power $P^*_{mn}$ is obtained by multiplying the incident in-duct power $P_{mn}$ by the the modal energy transmission coefficient $T_{mn}$ as shown in Equation (5). It should be noted that $T_{mn}$ does not depend on the type of noise source.

$$P^{*\,I/II}_{mn} = T_{mn} \cdot P_{mn}^{\;I/II} \tag{5}$$

A simple model using low- and high-frequency asymptotic solutions has been implemented to compute $T_{mn}$. The high-frequency solution for modes above cut-off was derived by Joseph [7]. It is given by Equation (6) where $\alpha_{mn}$ is the cut-on factor.

$$T_{mn} \rightarrow \frac{4 \cdot \alpha_{mn}}{(1+\alpha_{mn})^2} \tag{6}$$

The low-frequency solution for the plane wave is given in Equation (7) (see [8]). The value of $a$ is set so as to ensure continuity with the high-frequency solution.

$$T_{mn} \rightarrow a \cdot (kR)^2 \tag{7}$$

# 3 Results

A simulation was performed for a generic conventional fan with 18 rotor blades, 24 stator vanes and within the subsonic range of tip rotor speed.

## 3.1 Fan maps

Fig.4 shows the simulated fan map of aerodynamic efficiency. Fig.5 and 6 show the simulated noise maps of the free-field total sound power level for the tonal and broadband components, respectively.

These diagrams provide a straightforward view of the global acoustic behaviour of the fan over the whole range of operating conditions. Relating the noise maps to the aerodynamic map is part of the “design-to-noise” approach.

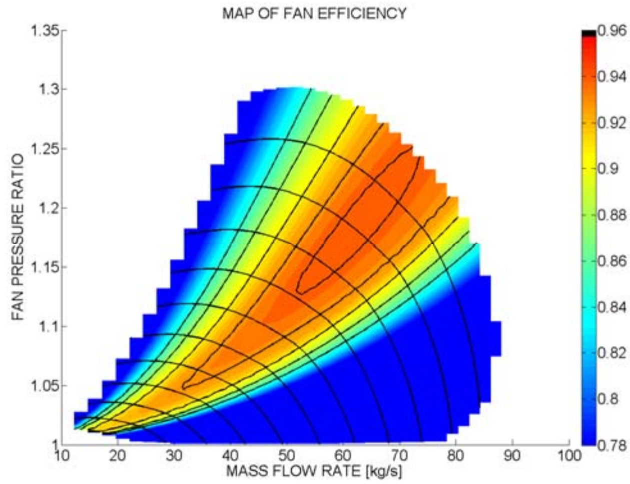


Fig.4: Map of fan aerodynamic efficiency.

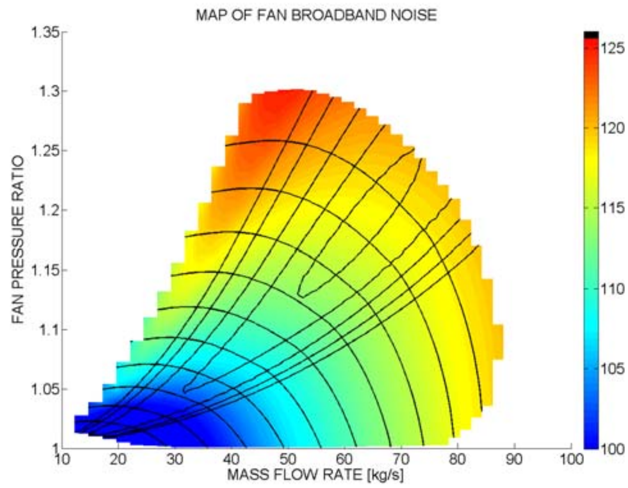


Fig.5: Map of fan broadband noise level (dB-scale).

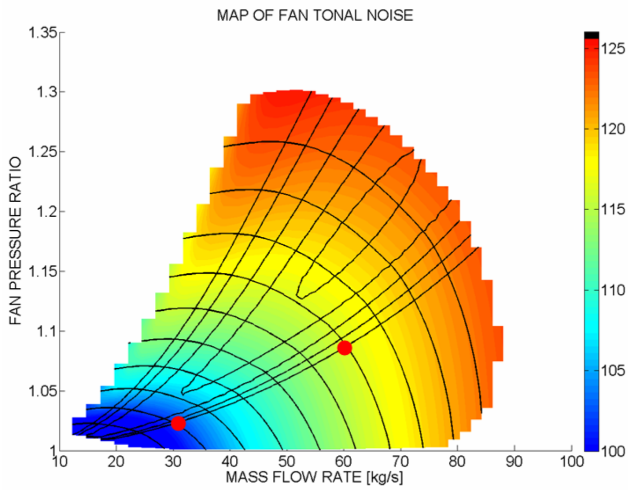


Fig.6: Map of fan tonal noise level (dB-scale).

## 3.2 Noise spectra

Noise spectra at the operating points identified in red in Fig.6 are shown here. The spectra include both tonal and broadband noise components. The black, red and blue lines depict the free-field generated spectrum, the in-duct spectrum and the far-field radiated spectrum, respectively. The typical resonance effects occurring near mode cut-off frequencies are clearly visible in the in-duct spectra. At high frequencies, the free-field and in-duct spectra of broadband noise coincide as the effects of duct confinement become negligible in that frequency domain.

At low fan speed ($M_{tip}$=0.25, Fig.7) the 1-BPF and 2-BPF tones do not show up in the in-duct spectra because no Tyler & Sofrin modes can propagate. This is a result of the so-called "cut-off design" of the fan. With the present 18-blade/24-vane configuration, the cut-off design is obtained only at low speeds. As fan speed increases the BPF-frequencies increase too, and the related Tyler & Sofrin modes can propagate (see spectra in Fig.8 for a medium fan speed case, $M_{tip}$=0.50).

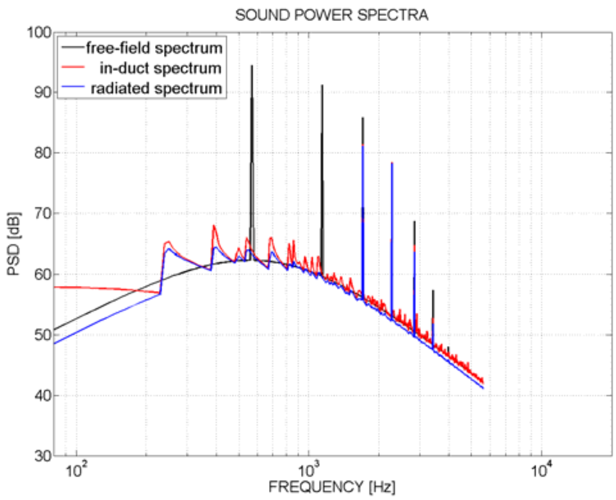


Fig.7: Noise spectra for $M_{tip}$=0.25.

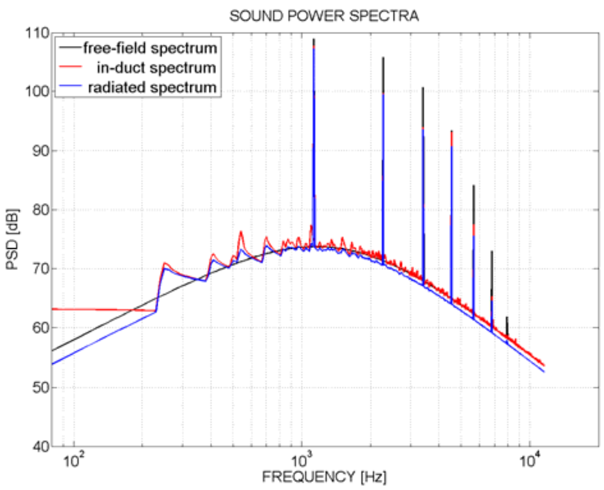


Fig.8: Noise spectra for $M_{tip}$=0.50.

## 3.3 Modal content

The following Figures 9, 10 and 11 depict some modal power distributions $P_{mn}$ of the sound field. The color-axis corresponds to the modal sound power, the x-axis to the mode azimuthal order *m* and the y-axis to the mode radial order *n*. The modal content of the 5-BPF tone is shown in Fig.9. The correlation of tonal sources leads to non-zero sound power solely for cut-on Tyler & Sofrin modes. Here, these are the modes of azimuthal orders -30, -6 and +18. All other propagating modes (in blue) carry zero sound power due to destructive vane-to-vane interferences. Fig.10 presents the modal content of broadband noise near the 5-BPF frequency. Given the uniform radial distribution of uncorrelated monopoles, the modes near cut-off turn out to be dominant. The transmitted part of the previous modal content is shown in Fig.11. With the model currently implemented (Eq. (6)) the termination has a significant effect only for modes near cut-off.

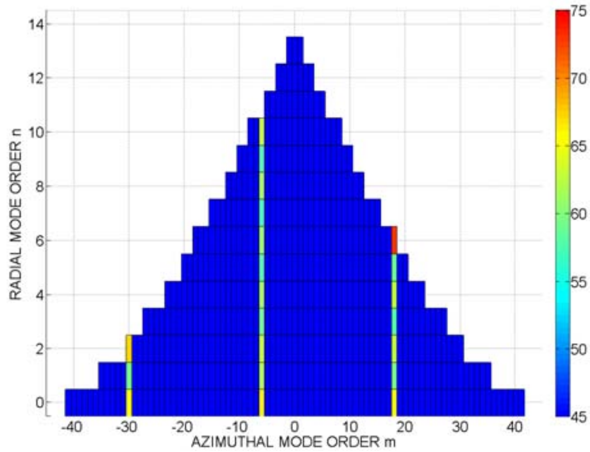


Fig.9: Modal content of the in-duct 5-BPF tone (dB-scale).

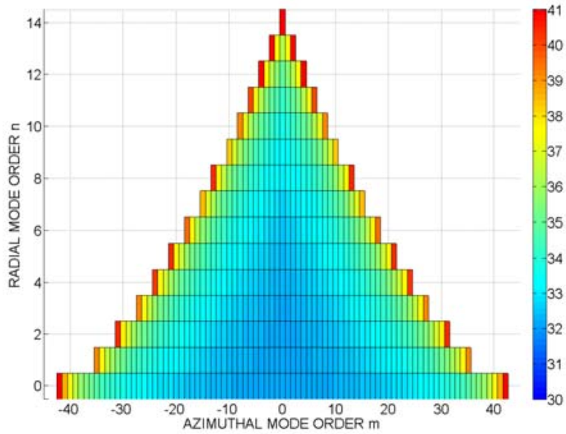


Fig.10: In-duct broadband modes (dB-scale).

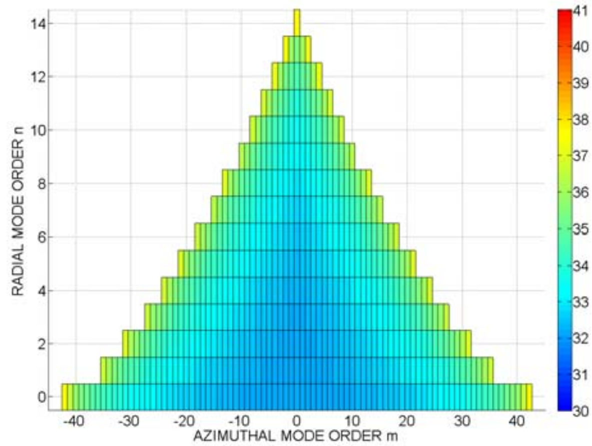


Fig.11: Transmitted broadband modes (dB-scale).

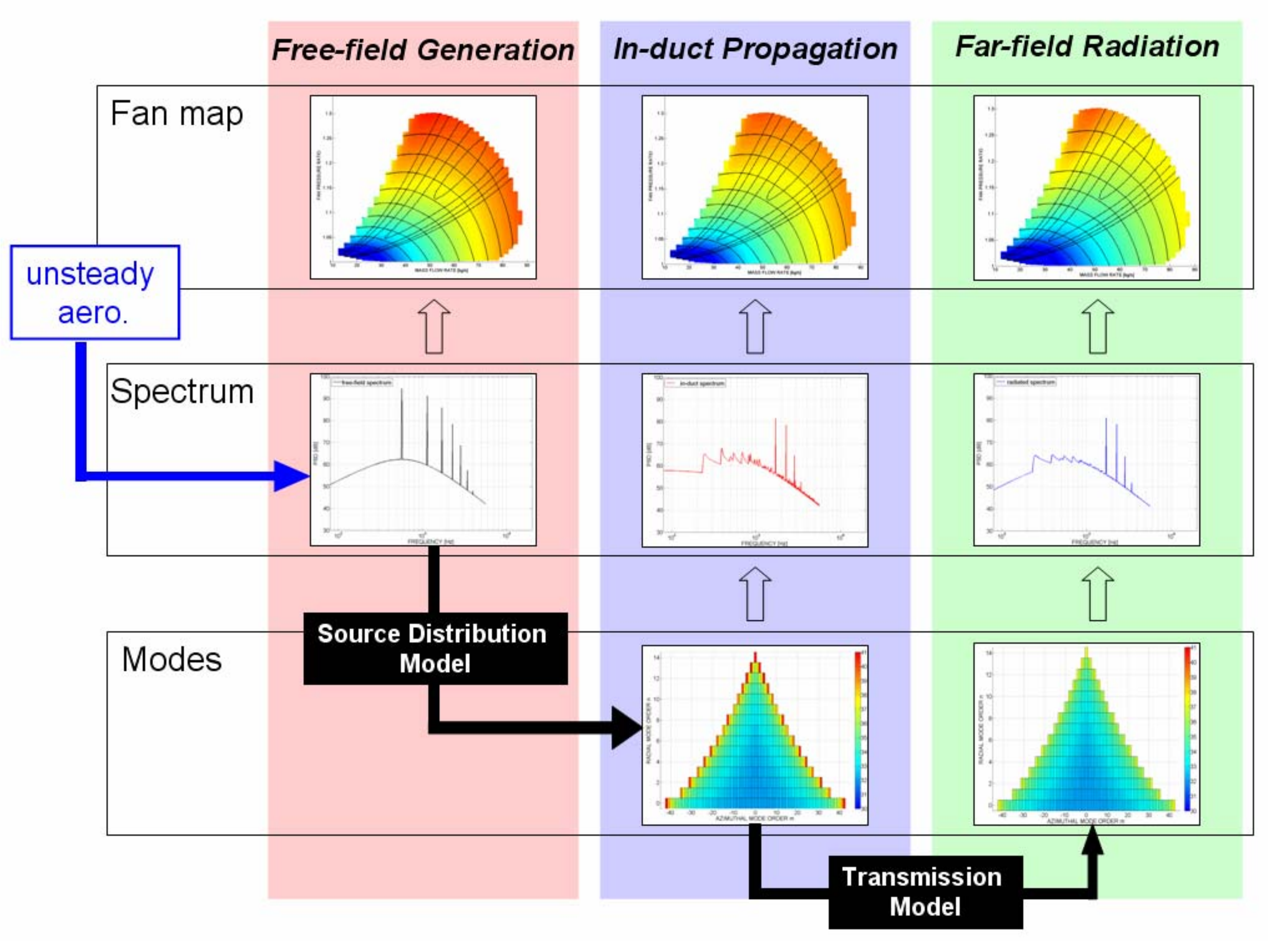


Fig.12: Computation steps from aerodynamic inputs to far-field acoustic results.

## 4 Summary and outlook

An improved version of a new prediction tool for fan noise has been implemented and tested. The different computation steps are schematically depicted in Fig.12. The "unsteady aero." module provides input parameters for the noise generation, which assumes non-interfering airfoils in free field. The interference effects due to the location of the sources relative to each other and the duct confinement are accounted for in the source distribution model. A detailed description of the sound field based on duct modes has been implemented and will be useful to investigate the effect of the different parts of the duct.

In addition to the transmission at the duct terminations modelled in the present study, future work will focus on assessing the liner performance and the transmission through a blade row. Further significant sources for fan noise such as rotor trailing edge noise and buzz-saw noise will also be implemented.

The work presented here forms the basis for a fan noise prediction tool that will be dedicated to the assessment of future engine concepts (contra-rotating fan, open rotor,…).

## References

[1] A. Moreau, L. Enghardt, "A first step towards a parametric model for fan broadband and tonal noise", DAGA, Conference Proceedings, Dresde 2008.

[2] M.F. Heidmann, "Interim prediction method for fan and compressor source noise", NASA technical memorandum X-71763, 1979.

[3] R.K. Amiet, "Acoustic radiation from an airfoil in a turbulent stream", Journal of Sound and Vibration, n°41, p.407-420, 1975.

[4] W.R. Sears, "Some aspects of non-stationary airfoil theory and its practical application", Journal of the Aeronautical Sciences, p.104-108, 1941.

[5] S. W. Rienstra, B.J. Tester, "An analytic Green´s function for a lined circular duct containing uniform mean flow", AIAA-2005-3020, 2005.

[6] J.M.Tyler, T.G. Sofrin, "Axial flow compressor noise studies", Society of Automotive Engineers Transactions, Vol. 70, p.309-322, 1962.

[7] P. Joseph, C.L. Morfey, "Multimode radiation from an unflanged, semi-infinite circular duct", J. Acoust. Soc. Am., n°105 (5), May 1999.

[8] P.O.A.L. Davies, "Reflection coefficient for an unflanged pipe with flow", Journal of Sound and Vibration, n°72, p.543-546, 1980.